ELSEVIER

Polymer 42 (2001) 2091–2100

polymer

www.elsevier.nl/locate/polymer

PNIPAAm and PMAA co-grafted porous PE membranes: living radical co-grafting mechanism and multi-stimuli responsive permeability

T. Peng, Y.-L. Cheng*

Department of Chemical Engineering and Applied Chemistry, University of Toronto, Toronto, Ontario, Canada M5S 3E5

Received 1 November 1999; received in revised form 28 April 2000; accepted 28 April 2000

Abstract

PNIPAAm and PMAA co-grafted porous PE membranes were prepared by a living radical, sequential photografting method, and shown to have a di-block covalent structure. In addition, DSC results suggest that complexes between the two blocks are formed under certain conditions. The effect of total co-graft yield and co-graft composition on the temperature- and pH responsive membrane permeability was examined. The results were explained using a two layer model, and by considering the effect of a graft conformation on the permeability of the individual layers. Finally, by imposing various combinations of temperature and pH, it was shown that the co-grafted membranes could be reversibly manipulated to exhibit more sophisticated permeability response than the singly grafted porous membranes. © 2000 Elsevier Science Ltd. All rights reserved.

Keywords: Living radical co-grafting; Responsive polymers; Responsive permeability

1. Introduction

Porous membranes with grafted responsive polymers have been extensively investigated [1–4]. In two previous studies, we reported that the graft yield and the location could significantly influence the temperature response of poly(*N*-isopropylacrylamide) grafted porous polyethylene membranes (PNIPAAm-*g*-PE), and the pH response of poly(methacrylic acid) grafted porous polyethylene membranes (PMAA-*g*-PE) [5,6]. Grafted polymer chains are primarily located within the pores of the membrane at low graft yields, and if a pore-wetting solvent is used during the grafting procedure. Alternatively, grafts on the external membrane surfaces may dominate if the graft yield is high and if a non-wetting grafting solvent is used. Permeation may thus be mainly controlled by either the pore layer or the surface layer, and the two mechanisms have opposite dependencies on graft conformations. Under pore-controlled conditions, expanded graft conformations result in reduced effective pore size, and therefore lower permeabilities relative to collapsed graft conformations. In contrast, under surface-controlled conditions, the expanded graft conformations represent greater degrees of hydration in the surface layer, and therefore give rise to higher permeabilities than the collapsed conformations.

The significance of polymers that respond to more than one environmental stimulus has been recognized [7–12]. These polymers are expected to provide more sophisticated responsiveness and greater potential for novel applications. For example, it has been stated that a hydrogel exhibiting swelling response to both pH and temperature could be used for drug delivery in conditions where the two are coupled such as blood clots [9]. However, the advantages of multi-stimuli responsiveness over single responsiveness in a clearly defined application remains to be demonstrated.

Two main approaches have been used to prepare multi-stimuli responsive polymers. One approach involves making interpenetrating polymer networks (IPN) of two polymers with independent stimuli-responsiveness. This method has been used to make IPNs composed of temperature-responsive poly(*N*-isopropylacrylamide), or PNIPAAm, and a pH-responsive hydrogel composed of either poly(acrylic acid) or poly(methacrylic acid) [13,14]. The method was also used to prepare hydrogels that showed biodegradation only in the presence of both enzymes for hydrolyzing each IPN component [10–12]. A second approach for making multi-stimuli responsive hydrogels is copolymerization of different responsive components. Random copolymer hydrogels of temperature-responsive PNIPAAm with pH-responsive comonomers are among the most studied [7,9,15].

Hydrogels composed of random linear copolymers of NIPAAm and a pH-responsive unit have been extensively studied. It has been found that the LCST or the temperature

* Corresponding author. Tel.: +1-416-978-5500; fax: +1-416-978-8605.
E-mail address: ylc@chem-eng.utoronto.ca (Y.-L. Cheng).

PII: S0032-3861(00)00369-4

responsiveness disappears at a high enough content of the pH-sensitive components, especially as the pH-sensitive units are ionized [7]. Block copolymers would contain long sequences of PNIPAAm and the pH-responsive component, that may result in hierarchical structures [16,17] or separated microphases [18,19] such that each responsive component can be independently activated by their respective stimulus. Therefore, block copolymers are more useful for multi-stimuli responsive applications than random copolymers.

By grafting multi-stimuli responsive block polymers onto a porous membrane, permeability can be controlled by more than one factor. Multiple architectures of the grafted chains can be designed leading to more control over the membrane permeability. In addition, depending on interactions between different blocks in response to stimuli, structures of the block copolymer may be tailored to regulate the membrane permeability.

Recently, a number of studies on the living free radical graft polymerization have been reported, which may provide new possibilities for preparing grafted block copolymers [20–24]. For example, by the combined use of Langmuir–Blodgett and atom transfer radical polymerization techniques, block copolymers grafted onto a membrane with precisely controlled architectures and densities have been obtained [23].

On the basis of the knowledge gained in our previous studies [5,6], the photochemical co-graft polymerization method was used to incorporate temperature and pH responsive polymers onto a porous membrane. To obtain the desired block structure, a sequential photografting procedure was devised based on a living free radical polymerization mechanism, which involves a reversible combination of growing polymer chains with stable free radicals. Living free radical polymerization has been widely investigated using different initiators called iniferters (derived from initiator–transfer agent–terminator) [25,26]. Photoiniferters, which initiate living free radical polymerization under UV irradiation, have been used to graft block copolymers onto membranes [20,24]. The photoiniferter may be either immobilized on the membrane or dissolved in the monomer solution. The photoiniferter generates free radicals at the surface that initiate polymerization, then stays at the end of the propagating chain, and retains the ability to initiate further polymerization, giving rise to living ends of the graft chains as the living graft polymerization proceeds.

In this study, the desired block co-grafts of PNIPAAm and PMAA on porous membranes were prepared using a living radical sequential grafting procedure. The effects of total co-graft yield and co-graft compositions on the membrane permeability were investigated.

2. Experimental

2.1. Materials

Low density polyethylene (LDPE) porous membranes produced via thermally induced phase separation were provided by 3M Company. The PE membrane is a flat sheet with 50.5 μm thickness, 70.5% porosity and an average pore diameter of 0.19 μm as specified by the manufacturer. *N*-isopropylacrylamide (NIPAAm) and photoinitiator xanthone were purchased from Aldrich Co. and used as received. Methacrylic acid (MAA), purchased from Polyscience Co., was purified by distillation under vacuum.

2.2. Graft polymerization

The grafting procedure has been described previously [5,6] and is therefore only briefly summarized here. 7 × 10.5 cm rectangular PE substrate membranes were soaked in acetone solution containing 0.3 wt% xanthone for 24 h and dried under vacuum at room temperature to prepare a xanthone-adsorbed film. PNIPAAm-*g*-PE membranes were prepared using a graft polymerization reactor under UV irradiation provided by a UV reactor as described previously [5]. A wide range of graft yields were obtained by varying UV irradiation time at a fixed monomer concentration of 0.22 M. To remove ungrafted homopolymers and residual photoinitiators, the membrane was washed in water at room temperature, and soxhlet extracted with methanol, then dried under vacuum. The process was repeated until constant dry weight was achieved. The NIPAAm graft yield was calculated as $(W_g - W_u)/W_u$ where W_u and W_g are the dry weights of the membrane before and after the PNIPAAm grafting, respectively. The membrane was soaked in methanol for 8 h, then in an aqueous MAA solution with a concentration of 0.22 M overnight. The graft polymerization was conducted using UV irradiation as described above. No additional photoinitiator was added prior to PMAA grafting. The grafted membrane was again subjected to repeated washing and drying process until the constant dry weight was achieved. The total co-graft yield was then calculated as $(W_{cog} - W_u)/W_u$ where W_u and W_{cog} are the dry weights of the membrane before and after co-grafting, respectively. The co-graft composition was calculated as the ratio between the dry weight of the PMAA graft and the total PNIPAAm and PMAA co-graft.

A number of 100% PNIPAAm and 100% PMAA-grafted membranes were also prepared for this study. The PNIPAAm-grafted membranes were prepared in the same way as described above. 100% PMAA-grafted membranes were prepared using a mixture of water and methanol (1:1 by volume) as the grafting solvent. The choice of solvent was made to promote PMAA grafting within the pores so that the graft locations would be comparable to PNIPAAm grafted membranes prepared in water [5,6].

2.3. Membrane characterization: differential scanning calorimetry (DSC) and thickness measurement

Co-grafted membranes with total co-graft yields of 410–472% and varying compositions were wetted in methanol and then equilibrated at pH 4.4 and 7.4 buffer at room

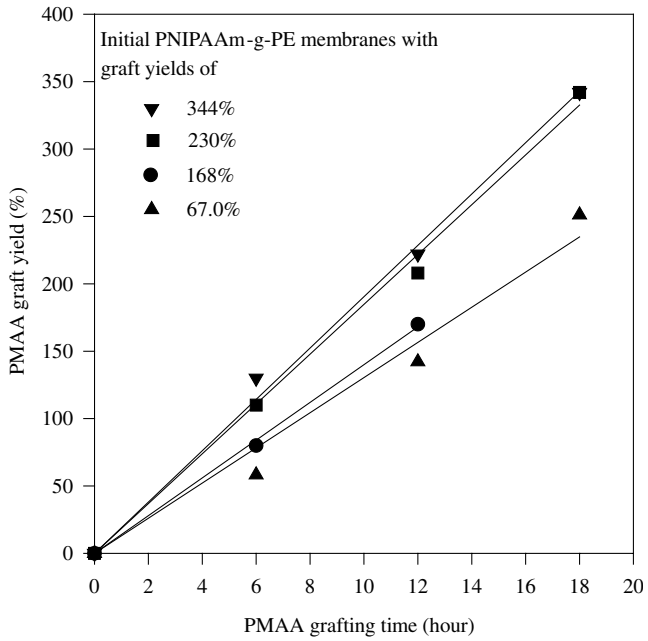

Fig. 1. Sequential photografting PMAA onto PNIPAAm-*g*-PE membranes ($n = 1$ for each data point).

temperature for two days. The membranes containing approximately 4 mg of grafted PNIPAAm were sealed in DSC pans and scanned in a Perkin–Elmer model 7 differential scanning calorimeter. The sample was heated at 5°C/min from 0 to 60°C under nitrogen against an empty reference pan. The temperature at the peak of a DSC thermogram is defined as the LCST.

Membrane thickness was measured at pH 4.4 and 7.4 buffer solution under 37 and 30°C using a micrometer with an accuracy of 0.01 mm. The relative membrane thickness was calculated as the ratio of the membrane thickness at pH 7.4, 30°C vs. at pH 4.4, 37°C.

2.4. Permeability measurement

Permeation experiments were carried out using the same permeation apparatus and method as before [5,6]. The grafted membranes were cut into discs and soaked first in methanol to wet the membrane and then equilibrated at 30°C, pH 7.4 and 37°C, pH 4.4 buffer solution with an ionic strength of 0.01 M prior to initiating permeation experiments. After checking for leakage, 25 ml of the buffer solution, and permeant solution in the same buffer were added simultaneously to the receptor and acceptor cells, respectively, and stirred with a pair of magnetic bars. A small amount (0.2 ml) of the solution was removed from the receptor cell at periodic time intervals, and solute concentration was determined by UV (Hewlett–Packard 8452Win Diode-array UV spectrophotometer). The sample was replaced with 0.2 ml blank buffer. Permeability was calculated using:

$$\ln(1 - 2C_r/C_0) = -2PAt/(LV)$$

where C_r is the concentration in the receptor cell at time t, and C_0, P, A, L and V are the initial solute concentration in the donor compartment, permeability, effective diffusion area, thickness of the membrane and volume of the compartment, respectively. The permeability coefficient P can be calculated from the slope of the $\ln(1 - 2Cr/C_0)$ versus t curve, which was determined by linear regression.

Dynamic permeation experiments were performed by changing both temperature and pH at certain time intervals. This was performed by transferring the permeation system between two water baths with temperatures of 37 and 30°C, and by changing pH buffer solutions in both the permeation cells simultaneously. A number of cycles were repeated, and the permeability under each condition in the cycle was calculated as described above.

3. Results and discussion

3.1. Co-grafting mechanisms and co-graft structure

The structure of PNIPAAm/PMAA co-grafts on porous PE membranes are of primary importance in determining the permeability characteristics of the grafted membranes. In the following sections, the primary and secondary structures of the co-grafts are discussed. The conclusions of Section 3.1 will serve as the basis for the discussion of permeation results in Section 3.2.

3.1.1. Co-grafting mechanism and co-graft primary structure

Fig. 1 shows the graft yield of PMAA onto PE membranes that had previously been grafted with PNIPAAm to varying extents as a function of grafting time. The figure shows that co-grafting can be achieved by this sequential procedure, and that PMAA graft yield increases with grafting time. The dependence of PMAA graft yield on grafting time is approximately linear, with an apparent slight acceleration with time. The co-graft composition can therefore be controlled by independently controlling PNIPAAm and PMAA grafting times.

The structure of the co-grafts produced by this procedure is of primary importance in determining the permeability response of these membranes. Clearly, the grafted PNIPAAm chains prepared by the sequential procedure must be attached to PE surfaces. Grafted PMAA chains, however, may theoretically be positioned either on the PE surfaces—giving independently grafted PNIPAAm and PMAA chains, or at the free ends of grafted PNIPAAm chains—giving PNIPAAm/PMAA di-block grafts. The sequential procedure was devised to create a di-block structure that would give rise to independent response of the two blocks. Xanthone is soluble in methanol (solubility = 4.9 mg/ml), so the methanol extraction step after PNIPAAm grafting should remove any residual photoinitiators adsorbed on PE surfaces, and prevent direct PMAA grafting

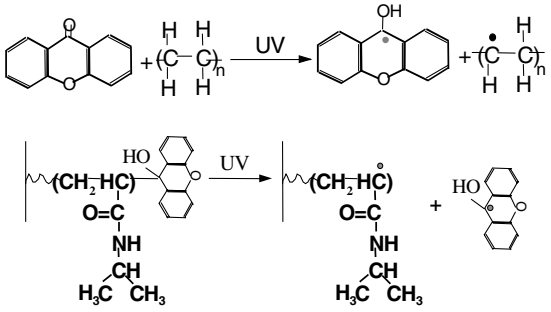

Fig. 2. Schematic illustration of the sequential grafting mechanism.

onto PE. No direct proof of complete xanthone removal was obtained due to the difficulty of identifying trace residual xanthone. However, a xanthone-coated PE membrane was extracted with methanol, neither PNIPAAm nor PMAA could be grafted—suggesting that the methanol extraction procedure was adequate for removing xanthone adsorbed on PE surfaces, and that the co-grafts have a di-block structure.

The literature on the living radical polymerization also supports the di-block structure idea. Yang et al. [24] have reported the living radical polymerization of PMAA on PE using xanthone. It was proposed that under UV irradiation, xanthone is excited and turns into xanthone ketyl radical after abstracting a hydrogen atom. The radical participates mainly in a termination process, resulting in grafted PMAA chains with terminal xanthone ketyl groups. Under further UV irradiation, the xanthone ketyl groups can decompose to form free radicals, leading to additional PMAA grafting. A similar mechanism may apply for PNIPAAm grafting and subsequent PMAA grafting, as shown in Fig. 2. Such a living radical polymerization mechanism would result in a di-block structure with the PMAA chains grafted at the free ends of PNIPAAm chains.

In Fig. 1, it can be seen that at equal PMAA grafting times, PMAA graft yield appears to be higher on membranes with higher PNIPAAm graft yields. An increase in PNIPAAm graft yield is obtained by increasing the UV irradiation time. Longer UV irradiation time should correspond to an increasing number of initiation events, and therefore a larger number of grafted PNIPAAm chains. Each of the PNIPAAm chains should have a living radical at its propagating end that can initiate subsequent PMAA grafting. Then in the PMAA grafting step, there should be a faster rate of PMAA grafting for the membrane with higher PNIPAAm graft yields.

Table 1
LCST of PNIPAAm and PMAA co-grafted membranes with different PMAA content at pH 4.4 and pH 7.4

PMAA (wt%)[a]	0	7.6	22.0	47.5	67.1
pH 7.4	32.3°C	33.8°C	31.3°C	31.1°C	30.6°C
pH 4.4	33.5°C	34.8°C	N.D.[b]	N.D.[b]	N.D.[b]

[a] The wt% is based on the total mass of grafted PMAA and PNIPAAm on each membrane. The membranes measured had total graft yields of 410–472%.

[b] Not detectable in the range of 0–60°C.

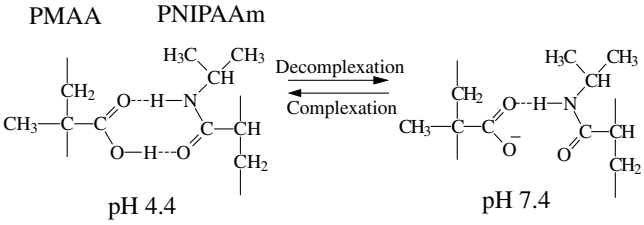

Fig. 3. Schematic illustration of reversible complexation between PNIPAAm and PMAA.

3.1.2. Secondary structure of PNIPAAm-co-PMAA-g-PE: complexation

It was argued in Section 3.1 that grafted membranes with di-block co-grafts of PNIPAAm and PMAA have been prepared. The LCST of membranes with varying compositions, and total graft yields in the range of 410–472%, were measured by DSC in order to determine the transitional temperatures of these co-grafts, as well as to probe their secondary structures. Table 1 shows that at pH 7.4, a thermal transition near the LCST of pure PNIPAAm occurs for membranes of all co-graft compositions. This observation further supports the idea that the co-grafts are di-block in structure, such that the PNIPAAm segments can undergo LCST transitions in much the same way that homopolymers of NIPAAm do. At pH 4.4, however, no LCST was detected within the temperature range of 0–60°C for membranes with a PMAA content of 22% or higher. A possible explanation for the disappearance of the LCST under these conditions is that at pH 4.4, hydrogen bonding between amide groups on PNIPAAm and un-ionized carboxyl groups on PMAA (Fig. 3) occurs, resulting in PNIPAAm/PMAA complexes. The LCST for PNIPAAm is a consequence of temperature-dependent changes in the balance between hydrophilic interactions in the form of hydrogen bonding between amide groups and water, and hydrophobic interactions among isopropyl groups. The shift in balance between these interactions results in a coil to globule conformational change in PNIPAAm chains [27,28]. The presence of a complex between PNIPAAm and PMAA may result in the loss of thermal transition because: (1) the amide groups of PNIPAAm are less accessible to water because of the hydrogen bonding with carboxylic acid groups—thus disrupting the balance between hydrophilic and hydrophobic interactions; and/or (2) the coil to globule conformational change of the PNIPAAm blocks is inhibited due to the more rigid structure of the complex.

The possible existence of PNIPAAm/PMAA complexes is supported by a number of literature reports [7,29–33]. Garay et al. reported that reversible intermolecular hydrogen bonding between PNIPAAm and poly(carboxylic acids), i.e. PMAA and PAA, in acidic solutions (i.e. pH $<$ pK_a) occurs, and

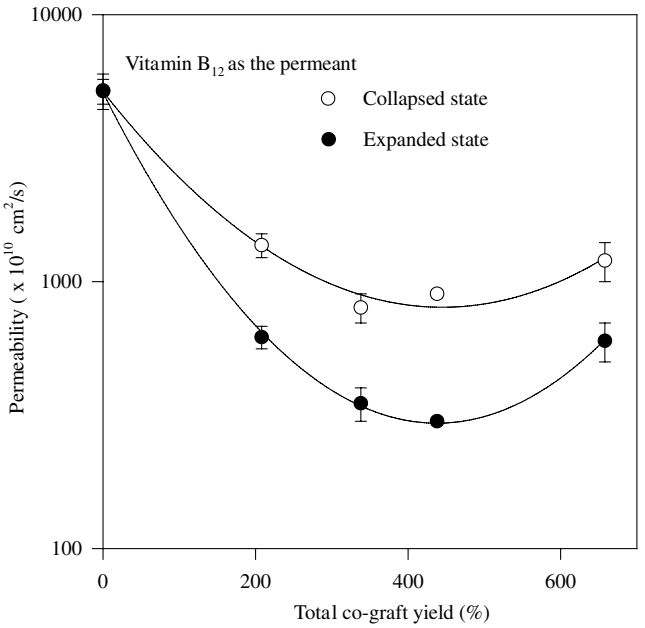

Fig. 4. Effect of total co-graft yield on vitamin B_{12} permeability through co-grafted membranes. All membranes contained 1:1 mass ratio of grafted PNIPAAm to grafted PMAA. Error bars are standard deviations ($n = 3$ pieces of the membrane from the same synthesis batch). The "expanded" condition corresponds to pH 7.4 and 30°C, and the nominally "collapsed" condition corresponds to pH 4.4 and 37°C.

that the hydrogen bonding results in solution precipitation [30]. Chen et al. reported that intramolecular hydrogen bonding between PNIPAAm grafts and PAA backbone chains in PAA-*g*-PNIPAAm copolymers occurs at pH 4 [7,29], and that these polymers show LCSTs close to that of PNIPAAm homopolymers at pH 7.4 over a wide range of compositions, while LCSTs are lowered at pH 4. It should be noted for comparison that in random copolymers of MAA and NIPAAm, the temperature responsiveness is lost at high enough MAA content both above and below the pK_a of the MAA groups [34].

3.1.3. Summary

In summary, the PNIPAAm-*b*-PMAA co-grafted membrane was obtained by sequential photografting of NIPAAm and MAA onto porous PE membranes. Hydrogen bonding between PNIPAAm and PMAA results in the formation of a complex under acidic condition. The complex structure results in the loss of the LCST for the PNIPAAm component. The structure of the co-grafts, together with total graft yield, composition and graft location, will influence membrane permeation characteristics. The permeation results presented in Section 3.2 will be discussed with these data in mind.

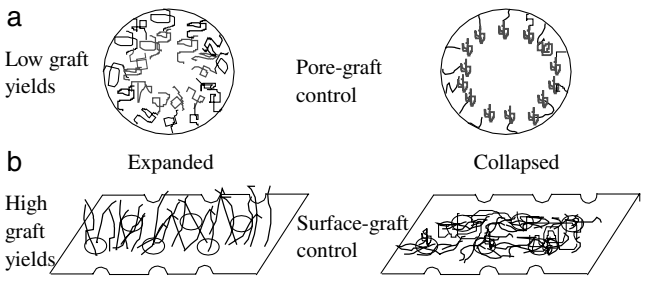

Fig. 5. Schematic illustration of two types of permeation control mechanisms.

3.2. Permeation characteristics of co-grafted membranes

In this section, the effect of total co-graft yield and co-graft composition on the membrane permeation characteristics are examined. Results are discussed in view of the co-graft structures discussed in the previous section, the membrane architecture that would result from those structures, as well as a two-layer membrane model. Finally, the possibility of multiple permeation set points is demonstrated.

3.2.1. Effect of total co-graft yield

Fig. 4 shows the permeability of vitamin B_{12} through co-grafted membranes as a function of total graft yield. The co-graft composition was maintained constant for all membranes—with a constant mass ratio of 1:1 for grafted PNIPAAm vs. PMAA. Permeation experiments were conducted under two conditions: (i) the "expanded" condition corresponding to pH 7.4 and 30°C when both the PNIPAAm and PMAA blocks of the co-grafts are expected to be in their expanded conformations, and (ii) the nominally "collapsed" condition corresponding to pH 4.4 and 37°C when both the PNIPAAm and PMAA blocks are expected to be in collapsed conformations—recognizing that complexes are likely to exist that may inhibit the collapse of PNIPAAm blocks. The figure shows: (1) permeability in the nominally collapsed state is always higher than in the expanded state; and (2) in both states, permeability first decreases with increasing co-graft yield, reaching a minimum, then increases as co-graft yield increases further.

The observed experimental results can be explained in terms of a two layer model. The grafted membranes may be viewed as being composed of two layers: the porous membrane layer that consists of the PE substrate with polymers grafted in its pores (pore grafts), and the surface layer that consists of polymers grafted on the external surfaces of the PE membrane (surface grafts) (Fig. 5). The overall permeability of the membrane, P, is related to the total thickness L, the permeability P_p and thickness L_p of the porous layer, and the permeability P_S and thickness L_S of the surface layer in the following manner [35]:

$$\frac{L}{P} = \frac{L_p}{P_p} + \frac{L_S}{P_S}$$

The thickness of the porous layer, L_p, is approximately constant and equal to the thickness of the native PE substrate, while the surface layer thickness L_S increases

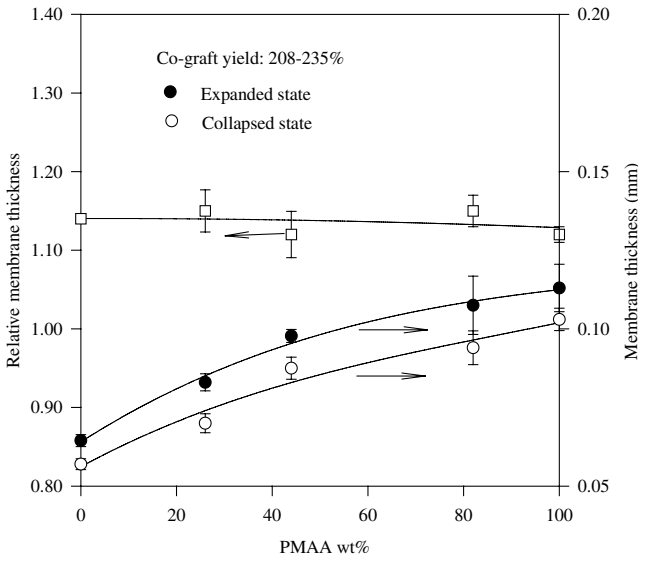

Fig. 6. Relative membrane thickness (□) and absolute membrane thickness (●, ○) as a function of PMAA content. Error bars are standard deviations($n = 4$ pieces of the membrane from the same synthesis batch).

with total graft yield. The permeability of the surface layer P_S should be comparable to the permeability of a corresponding PNIPAAm/PMAA copolymer hydrogel membrane, while the pore layer permeability P_p should decrease with increasing graft yield as pores become increasingly filled. The overall permeability may therefore be controlled by either the surface layer, the pore layer, or both, depending on the graft yield and location. The two layer model has been used previously to explain permeability results obtained in temperature-responsive PNIPAAm-*g*-PE membranes [5] and pH-responsive-PMAA-*g*-PE membranes [6]; in those studies, direct evidence for the existence of two layers were provided by thickness measurements as well as SEM photographs of the membrane cross-sections and surfaces.

Due to the large pore surface area, it is expected that at low total graft yields, the co-grafts would primarily be located inside the pores with only a small amount of grafting on the external surface ($L_S \approx 0$); the porous layer should therefore be the rate-controlling layer. Under these circumstances, as graft yield increases, increasing blockage of the pores would result, giving rise to decreasing permeability as seen in Fig. 4. Fig. 4 shows that at low yields, permeability in the nominally collapsed state is higher than in the expanded state. Expanded graft conformations lead to greater obstruction of the pores, and thus lower permeabilities than the collapsed conformations. Note that although complexation between PNIPAAm and PMAA blocks is expected at pH 4.4 and 37°C, the complex should have a tighter, denser conformation than the expanded conformations, and would therefore provide less blockage of the pores.

As the graft yield increases, the pores would eventually become filled, and an increasingly significant surface layer would be formed; the overall permeability would then become increasingly influenced by the permeability of the surface layer. It should be noted that the permeability used in this paper refers to the thickness-normalized intrinsic permeability of the membranes or layers within the membranes. The intrinsic permeability of the surface layer should not be significantly thickness dependent, and should be close to that of a slightly crosslinked hydrogel. The intrinsic permeability of the porous layer should be lower than that of the surface layer. Then as the surface layer thickness increases, the relative importance of the surface layer in determining the overall permeability increases, and the overall intrinsic permeability increases as a result. This expected trend with respect to graft yield is observed in Fig. 4 for both the expanded state and the nominally collapsed state. If at sufficiently high graft yields, the surface layer becomes so thick that it becomes completely rate-controlling, then the overall permeability would be the same as that of a hydrogel membrane. In this situation, the nominally collapsed conformation would present a denser barrier to diffusion than the expanded conformation, and a lower permeability would be expected for the collapsed state. In Fig. 4, permeability in the expanded state is always lower than in the collapsed state, suggesting that the surface layer-controlled limit is never reached within the range of experimental conditions tested. However, the difference in permeability between the two states appears to be getting smaller with increasing graft yield in the high graft yield range, suggesting that the surface layer-control limit would eventually be approached at higher graft yields.

3.2.2. Effect of co-graft composition

The effect of co-graft composition on permeability was studied at two different ranges of total co-graft yields: 208–235% and 410–472%; the two ranges were selected to represent membranes with varying degrees of pore layer vs. surface layer control.

The thicknesses and permeation characteristics of the lower graft yield range membranes are shown in Figs. 6 and 7. Thickness measurements and permeation experiments were conducted under conditions that represent either fully expanded conformations (30°C, pH 7.4) or nominally collapsed conformations (37°C, pH 4.4). The ratio of thicknesses between these two conformational states is defined as the relative membrane thickness. In Fig. 6, it can be seen that the absolute thicknesses of the membranes are larger than the ungrafted PE substrates (0.05 mm), the membranes are thicker in the expanded state compared to the collapsed state, resulting in values that are larger than one for the relative thicknesses between expanded and collapsed states. These observations indicate that some grafts exist on the external membrane surfaces. It can also be seen that although relative thickness is nearly composition-independent, absolute membrane thickness increases with increasing PMAA content. This may indicate that the PMAA grafts are preferentially grafted onto the external

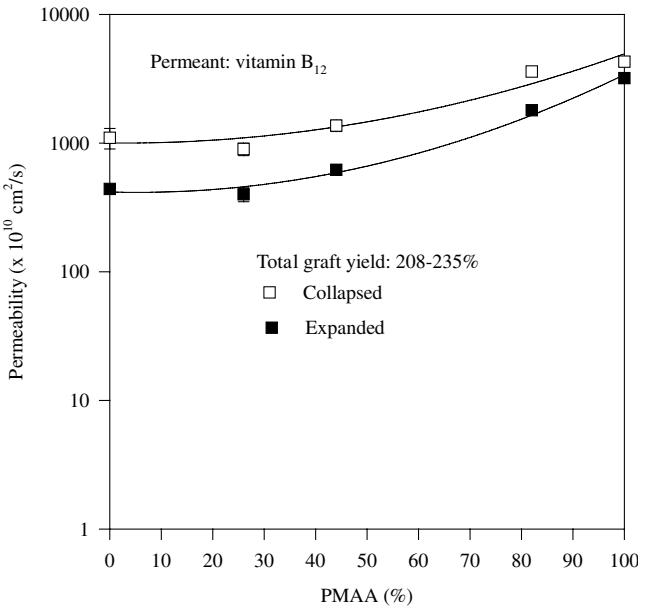

Fig. 7. Effect of co-graft composition on the permeability of the membrane with 208–235% total co-graft yields. Error bars are standard deviations ($n = 3$ pieces of the membrane from the same synthesis batch). The "expanded" condition corresponds to pH 7.4 and 30°C, and the nominally "collapsed" condition corresponds to pH 4.4 and 37°C.

surfaces compared to the PNIPAAm grafts. Due to the sequential photografting procedure, a higher PMAA content, or lower PNIPAAm content, means that surface adsorbed xanthone photoinitiator is removed from the pore surfaces at a lower partial graft yield, and therefore, a higher amount of polymer is subsequently attached onto the end of previously grafted chains via a living radical mechanism. This situation would result in a higher proportion of grafted polymers on the membrane surface with increasing PMAA content.

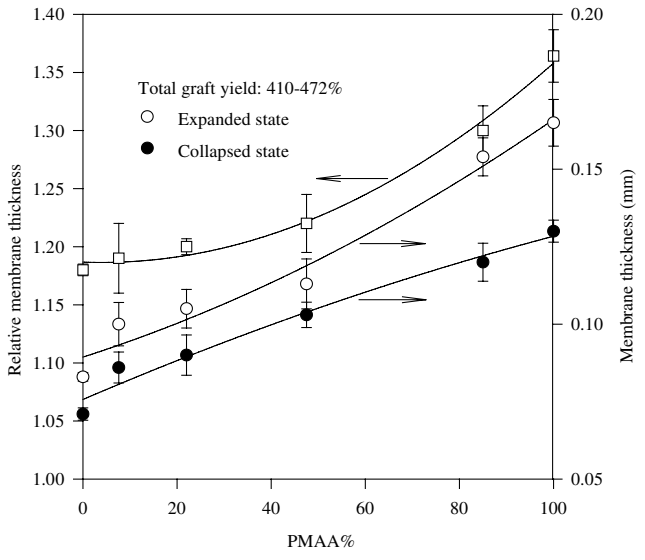

Fig. 8. Relative membrane thickness (□) and absolute membrane thickness (○, ●), as a function of PMAA content. Error bars are standard deviations ($n = 4$ pieces of the membrane from the same synthesis batch).

Fig. 7 shows the permeability of vitamin B_{12} through the low graft yield range membranes as a function of PMAA content. It can be seen that permeability in the collapsed state is always higher than in the expanded state. Since at this graft yield range, pore layer control is expected to be important, the expanded grafts would obstruct pores more than the collapsed grafts, and would therefore lead to lower permeabilities. Fig. 7 also shows that permeability increases with the PMAA content for both collapsed and expanded graft conformations. Since, as described earlier, increasing PMAA content represents increasing amounts of graft on the external surface, there would be correspondingly less grafts in the pores, leading to reduced pore obstruction, and therefore higher overall permeability.

The thicknesses and permeation characteristics of the higher graft yield range membranes are shown in Figs. 8 and 9. Fig. 8 shows that these membranes are thicker than ungrafted PE membranes (0.05 mm), and are thicker in the expanded state than the collapsed state. The same observation was seen in Fig. 6 for the lower graft yield membranes, and can similarly be attributed to the presence of grafts on the external membrane surfaces. Comparison of Figs. 6 and 8 shows that the higher graft yield membranes are thicker than the lower graft yield membranes, as would be expected. It can also be seen that absolute membrane thicknesses, as well as the relative membrane thickness between the expanded and collapsed states, both increase with increasing PMAA content. As discussed earlier, due to the procedure used to prepare co-grafts, PMAA is expected to be more localized on the external surfaces than PNIPAAm, therefore thicker surface layers are expected with increasing PMAA content. An additional factor may influence thickness at the higher graft yields: there may be a significant presence of PNIPAAm on the external surface at these yields; the composition of the surface layer may influence membrane thickness, and thus result in a dependence of thickness on the overall PMAA content. In studies of PNIPAAm and PMAA grafted dense membranes [36,37], as well as PMAA and PNIPAAm hydrogels of similar crosslinking densities [9,38,39], swelling ratios of the two polymers in their collapsed and expanded states are seen to be comparable. These literature reports suggests that surface layer composition should not have a strong effect on overall membrane thickness, and the PMAA dependence seen in Fig. 8 should simply be attributed to the increasing localization of grafts in the surface layer with increasing PMAA content.

Fig. 9 shows the permeability of vitamin B_{12} through co-grafted membranes with the higher range of co-graft yields under fully expanded and nominally collapsed conditions. It is observed: (1) in both expanded and collapsed states, permeability increases with PMAA content; and (2) at low PMAA contents, permeability in the collapsed state is lower than in the expanded state, but the trend reverses as PMAA

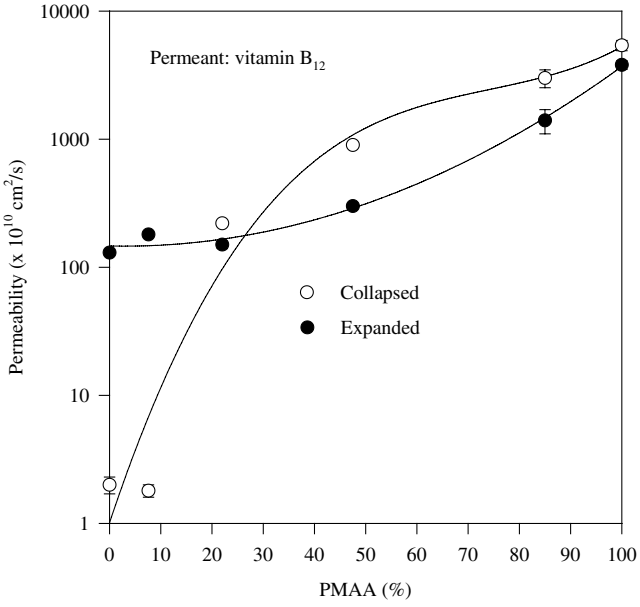

Fig. 9. Effect of PMAA content on the permeability of the co-grafted membrane with 410–472% total graft yields. Error bars are standard deviations ($n = 3$ pieces of the membrane from the same synthesis batch). The "expanded" condition corresponds to pH 7.4 and 30°C, and the nominally "collapsed" condition corresponds to pH 4.4 and 37°C.

content increases. These observations can be most readily explained by first examining the permeability of the surface and porous layers individually. It may be argued that since the surface layer is composed of only hydrated grafts, the surface layer permeability should be comparable to the permeability of a corresponding hydrogel membrane. Data from the literature on diffusion coefficients of rhodamine, and partition coefficients and permeability of vitamin B_{12} through PNIPAAm and PMAA hydrogels of comparable crosslinking density [40–42] allowed calculations to be made that showed vitamin B_{12} permeability through expanded PNIPAAm and PMAA hydrogels have comparable values of about 10^{-6} cm^2/s, while permeability through the collapsed PNIPAAm ($\sim 10^{-9}$ cm^2/s) is orders of magnitude lower than through the collapsed PMAA ($\sim 10^{-6}$ cm^2/s). This trend in permeability is qualitatively consistent with known volume changes for these two hydrogels between their swollen and collapsed state [41]. Thus permeability of the surface layer either remains constant (expanded state) or increases (collapsed state) with increasing PMAA content. In addition, the permeability data for low graft yield membranes shown in Fig. 7 can be used to infer that pore layer permeability should be of the order of magnitude 10^{-8} to 10^{-7} cm^2/s, and should increase with PMAA content due to the preferential localization of PMAA grafts on external surfaces. Fig. 10 schematically shows the PMAA dependence of permeability for the two layers in both conformations.

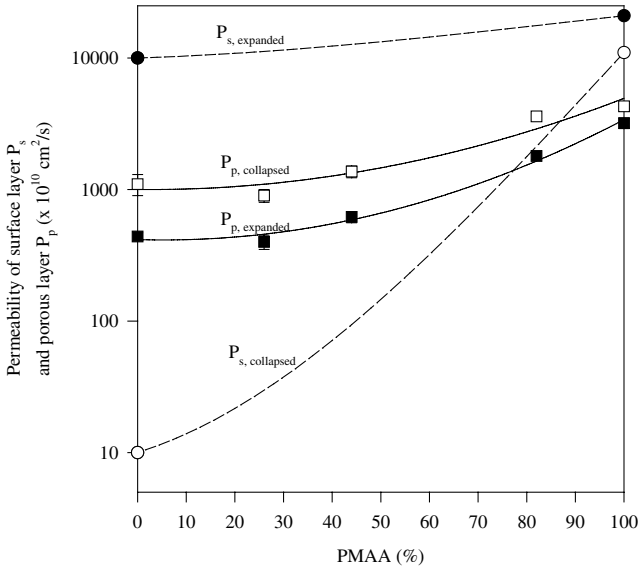

Fig. 10. Schematic illustration of the effect of PMAA content on the permeability of the pore layer and the surface layer. The magnitudes of permeability are estimated from either reference sources [40–42] or Fig. 7, as discussed in the text.

Looking at the combined effects of the pore and surface layers shown in Fig. 10, it is readily apparent that as PMAA content increases, the overall membrane permeability in both the expanded and collapsed states must increase, as was observed in Fig. 9. In addition, membrane permeability in the expanded state should increase only moderately with PMAA content, only due to the effect of increasing PMAA on the pore layer. In contrast, in the collapsed state, permeability of the pore layer increases moderately while permeability of the surface layer increases dramatically—resulting in a significant increase in overall permeability with PMAA content. The difference in the effect of PMAA content on overall membrane permeability in the expanded and collapsed state results in the crossover seen in Fig. 9.

It is also of interest to note that the crossover in Fig. 9 occurs at around 22% PMAA—the same co-graft composition at which the LCST transition became undetectable by DSC (Table 1). If the surface layer is prevented from collapsing due to complexation between PNIPAAm and PMAA, then permeability through the surface layer should be significantly higher than if collapse could occur. The marked increase in the permeability in the collapsed conformation between 7.6 and 22% PMAA may therefore be attributed to complex formation.

3.2.3. Responsive membrane with multiple permeability set points

To demonstrate the range of permeability control achievable with multi-stimuli responsive membranes, permeation experiments were conducted by randomly changing the pH and temperature among four different conditions that represent the possible combinations of the collapsed or expanded conformations for PNIPAAm and PMAA: (30°C/pH 7.4), (37°C/pH 7.4), (30°C/pH 4.4), and (37°C/pH 4.4). Experiments were conducted using 4400 dalton FITC-dextran

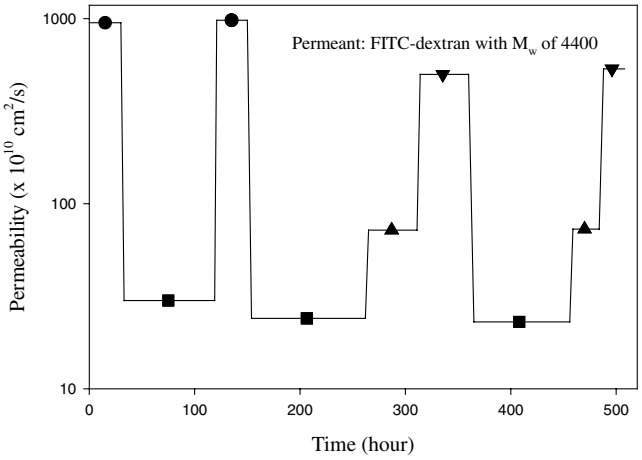

Fig. 11. Dynamic permeability changes of a membrane with total graft yield of 208% and 1:1 mass ratio of grafted PNIPAAm to PMAA in response to both temperature and pH changes. (●) pH4.4, 37°C; (■) pH7.4, 30°C; (▲) pH7.4, 37°C; (▼) pH4.4, 30°C.

since more dramatic permeability changes are expected for solutes of this size than vitamin B_{12} [5,6]. Two membranes were used, each with a PNIPAAm to PMAA ratio of 1:1, and with two different total co-graft yields of 208 and 438%. The results (Figs. 11 and 12) show that permeability can be controlled in a reversible fashion, and that there are four permeability set points for each membrane corresponding to the four different conditions, demonstrating that a more sophisticated permeability response can be obtained by co-grafted membranes than membranes grafted with only a single stimulus-responsive polymer. The response times, after new conditions were imposed, were not quantitatively determined, but permeation results show that a new steady state had generally been reached at the typical first time point of 2 h after changing conditions.

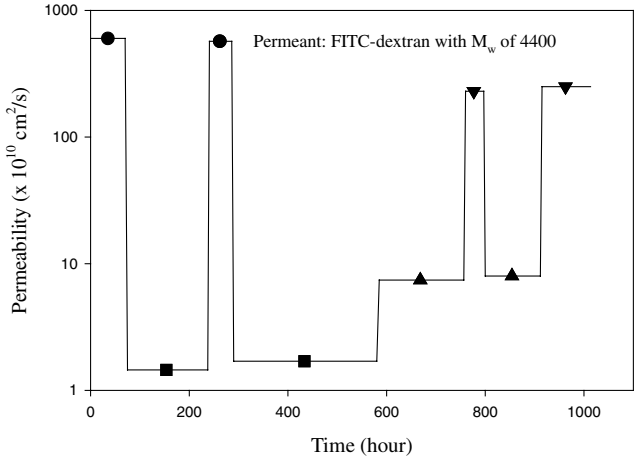

Fig. 12. Dynamic permeability changes of a membrane with total graft yield of 438% and 1:1 mass ratio of grafted PNIPAAm to PMAA in response to coupled temperature and pH changes. (●) pH4.4, 37°C; (■) pH7.4, 30°C; (▲) pH7.4, 37°C; (▼) pH4.4, 30°C.

Figs. 11 and 12 also show that for both membranes, the permeabilities can be ranked in the following order: $P_{(37°C/pH\ 4.4)} > P_{(30°C/pH\ 4.4)} > P_{(37°C/pH\ 7.4)} > P_{(30°C/pH\ 7.4)}$. At 30°C, pH 7.4, both PNIPAAm and PMAA blocks are fully expanded, giving the largest possible co-graft chain dimensions, and the lowest permeability if the overall membrane permeability is governed by the pore layer. At 37°C, pH 7.4, PNIPAAm blocks collapse, showing the LCST, while PMAA blocks are expanded. At 30°C, pH 4.4, complexes are present. The hydrophilic groups in the co-grafted polymer (i.e. amide and carboxylic acid groups) involved in the hydrogen bonding are no longer available for water molecules. The complex should have a tighter, denser conformation than the partially expanded conformation at 37°C and pH 7.4. At 37°C, pH 4.4, the structure of the complex becomes even more compact due to increased hydrophobic interaction between the methyl groups of PMAA and isopropyl groups of PNIPAAm with temperature [31,33]. The rank order in permeability for the various conditions therefore correlates inversely to the expected graft chain dimensions, implying that for both membranes, the pore layer is a strong determinant of the overall permeation characteristics. Although it is expected that the surface layer should play a larger role in determining the permeation characteristics of the higher graft yield membrane than the lower graft yield membrane, the complexation that occurs at pH 4.4 reduces the extent of collapse possible in the surface layer, thus minimizing the mass transfer resistance and the degree of mass transfer control of the surface layer. Nevertheless, since grafted chain conformations have an opposite effect on the permeability of pore layer vs. the surface layer, differences in the degree of control exerted by the pore layer would ultimately be manifested in a different rank order in permeability. Further comparison of Figs. 11 and 12 show that, although the rank orders in permeabilities are the same for the two membranes, the actual values of permeabilities are different for the two membranes under the same conditions—an indication of the shift in the degree of pore layer control.

4. Conclusions

Membrane preparation, co-graft structure and permeation characteristics have been studied with the following conclusions:

1. Both temperature and pH responsive membranes with a wide range of co-graft yield and composition can be prepared by the sequential photografting method. The process shows living radical polymerization characteristics leading to a di-block co-graft structure.
2. The co-grafted membrane with the PMAA content ranging from 7.6 to 67.1 wt% shows the LCST at pH 7.4. In contrast, the co-grafted membrane with the PMAA content above 22 wt% shows no LCST at pH

4.4 due to complexation between PMAA and PNIPAAm blocks.

3. The permeability of the co-grafted membrane is controlled by the co-graft architecture which, in turn, is affected by the total co-graft yield and co-graft composition.
4. More sophisticated permeability response behavior is possible with multi-stimuli responsive membranes than membranes that can respond to only one stimulus.

References

[1] Peng, T. PhD thesis, University of Toronto, 1999.
[2] Osada Y, Honda K, Ohta M. J Membr Sci 1986;27:327.
[3] Okahata Y, Noguchi H, Seki T. Macromolecules 1986;19:494.
[4] Ito Y, Kotera S, Inaba M, Kono K, Imanishi Y. Polymer 1990;31:2157.
[5] Peng T, Cheng Y-L. J Appl Polym Sci 1998;70:2133.
[6] Peng T, Cheng Y-L. J Appl Polym Sci 2000;76:778.
[7] Chen G, Hoffman AS. Nature 1995;373:49.
[8] Hoffman AS. Macromol Symp 1995;98:645.
[9] Brazel CS, Peppas NA. Macromolecules 1995;28:8016–20.
[10] Kurisawa M, Terano M, Yui N. Macromol Rapid Commun 1995;16:663.
[11] Yamamoto N, Kurisawa M, Yui N. Macromol Rapid Commun 1996;17:313.
[12] Kurisawa M, Yui N. Macromol Chem Phys 1998;199:1547.
[13] Shin BC, John MS, Lee HB, Yuk SH. Eur Polym J 1998;34:1675.
[14] Zhang J, Peppas NA. Polym Prepr 1998;39(2):228.
[15] Feil H, Bae YH, Feijen J, Kim SW. Macromolecules 1992;25:5528.
[16] Ikkala O, Ruokolainen J, ten Brinke G. Polym Prepr 1999;40(1):448.
[17] Ruokolainen J, Makinen R, Torkkeli M, Makela T, Serimaa R, ten Brinke G, Ikkala O. Science 1988;280:557.
[18] Mikosch W, Geissler E. Ber Bunsenges Phys Chem 1998;102:1589.
[19] Bates FS. Science 1991;251:898.
[20] Higashi J, Nakayama Y, Marchant RE, Matsuda T. Langmuir 1999;15:2080.
[21] Husseman M, Malmstrom EE, Mcnamara M, Mate M, Mecerreyes D, Benoit DG, Hedrick JL, Mansky P, Hung E, Russell TP, Hawker CJ. Macromolecules 1999;32:1424.
[22] Huang X, Wirth MJ. Macromolecules 1999;32:1694.
[23] Ejaz M, Yamamoto S, Ohno K, Tsujii Y, Fukuda T. Macromolecules 1998;31:5934.
[24] Yang W, Ranby B. Macromolecules 1996;29:3308.
[25] Otsu T, Matsumoto T. Adv Polym Sci 1998;36:75.
[26] Sebenik A. Prog Polym Sci 1998;23:875.
[27] Lin SY, Chen KS, Chu LR. Polymer 1999;40:2619.
[28] Wu C, Qiu X. Phys Rev Lett 1998;80:620.
[29] Chen G, Hoffman AS. Macromol Rapid Commun 1995;16:175.
[30] Garay MT, Llamas M, Iglesias E. Polymer 1997;38:5091.
[31] Staikos G, Karayanni K, Mylonas Y. Macromol Chem Phys 1997;198:290.
[32] Staikos G, Bokias G, Karayanni K. Polym Int 1996;41:345.
[33] Koussathana M, Lianos P, Staikos G. Macromolecules 1997;30:7798–802.
[34] Zhou S, Chu B. J Phys Chem 1998;102:1364.
[35] Kesting RE. Synthetic polymeric membranes: A structure perspective. New York: Wiley, 1985. p. 277.
[36] Kondo T, Kubota H, Katakai R. Eur Polym J 1998;34:1099.
[37] Kubota H, Nagaoka N, Katakai R, Yoshida M, Omichi H, Hata Y. J Appl Polym Sci 1994;51:925.
[38] Quinn TM, Grodzinsky AJ. Macromolecules 1993;26:4332.
[39] Hoffman AS, Afrassiabi A, Dong LC. J Controlled Release 1986;4:213.
[40] Kato E, Murakami T. Polym Gel Net 1998;6:179.
[41] Palasis M, Gehrke SH. J Controlled Release 1992;18:1.
[42] Turner J, Cheng Y-L. J Membr Sci 1998;148:207.